Cone beam computed tomography-based models versus multislice spiral computed tomography-based models for assessing condylar morphology

Liliane Rosas Gomes, DDS, MS, PhD,[a,b] Marcelo Regis Gomes, DDS,[c] João Roberto Gonçalves, DDS, MS, PhD,[a] Antônio Carlos O. Ruellas, DDS, MS, PhD,[d] Larry M. Wolford, DMD,[e] Beatriz Paniagua, PhD,[f] Erika Benavides, DDS, MS, PhD,[g] and Lúcia Helena Soares Cevidanes, DDS, MS, PhD[b]

Objective. To quantitatively compare condylar morphology using cone beam computed tomography (CBCT) and multislice spiral computed tomography (MSCT) virtual three-dimensional surface models.

Study Design. The sample consisted of secondary data analyses of CBCT and MSCT scans obtained for clinical purposes from 74 patients treated with condylar resection and prosthetic joint replacement. Three-dimensional surface models of 146 condyles were constructed from each scan modality. Across-subject models were approximated and voxel-based registration was performed between homologous CBCT and MSCT images, making it possible to create average CBCT- and MSCT-based condylar models. SPHARM-PDM software provided matching points on each corresponding model. ShapeAnalysisMANCOVA software assessed statistically significant differences between observers and imaging modalities. One-sample t-tests evaluated the null hypothesis that the mean differences between each CBCT- and MSCT-based model were not clinically significant (<.5 mm). Tests were conducted at a significance level of $P < .05$.

Results. ShapeAnalysisMANCOVA showed no statistically significant difference between the average CBCT- and MSCT-based models ($P > .68$). During pairwise comparison, the mean difference observed was .406 mm (SD, .173). One sample t-test showed that mean differences between each set of paired CBCT- and MSCT-based models were not clinically significant ($P = .411$).

Conclusion. Three-dimensional surface models constructed from CBCT images are comparable to those derived from MSCT scans and may be considered reliable tools for assessing condylar morphology. (Oral Surg Oral Med Oral Pathol Oral Radiol 2016;121:96-105)

Since the introduction of the cone-beam computed tomography (CBCT) imaging modality into dentistry in 1998,[1] this exam has undergone rapid evolution and has become an increasingly important source of three-dimensional (3-D) volumetric information for defining normal and abnormal anatomy of craniofacial structures.[2] CBCT images have assumed a prominent role in the diagnosis of temporomandibular joint (TMJ) dysfunction, particularly for assessment of morphologic changes in mandibular condyles presenting with osteoarthritis (OA).[3] CBCT has been shown to render high-resolution images providing a clear visualization of the hard tissues of the TMJ[3-5] and markedly reduces radiation and cost compared with multislice spiral computed tomography (MSCT).[1,4,6-8]

CBCT scans provide isotropic voxels (*i.e.,* equal dimension in height, width, and depth), which easily allow a multiplanar reconstruction without loss of spatial resolution.[9-12] Voxel sizes in CBCT imaging range from .076 mm to .4 mm, depending on the protocol being

Statement of Clinical Relevance

Cone beam computed tomography (CBCT)-based condylar models are reliably comparable to multislice spiral computed tomography (MSCT). The CBCT images lower radiation dose and cost provide clinicians and researchers with a valuable diagnostic tool for identifying specific osteoarthritic changes in the mandibular condyles such as erosion, flattening, and osteophytosis.

Supported by the National Institute of Dental & Craniofacial Research and the National Institute of Biomedical Imaging and Bioengineering of the National Institutes of Health (award number R01 DE024450) and by the Sao Paulo Research Foundation (FAPESP, Brazil, Grant 2013/22417-0). The content is solely the responsibility of the authors and does not necessarily represent the official views of the National Institutes of Health and FAPESP.

[a]Department of Orthodontics, Faculdade de Odontologia de Araraquara, UNESP Universidade Estadual Paulista, Sao Paulo, Brazil.
[b]Department of Orthodontics, School of Dentistry, University of Michigan, Ann Arbor, MI, USA.
[c]Private practice, Salvador, BA, Brazil.
[d]Department of Orthodontics, Universidade Federal do Rio de Janeiro, Rio de Janeiro, Brazil.
[e]Departments of Oral and Maxillofacial Surgery and Orthodontics Texas, A&M University Health Science Center Baylor College of Dentistry, Baylor University Medical Center, Dallas, TX, USA.
[f]Research Assistant Professor at the Department of Psychiatry, University of North Carolina, Chapel Hill, NC, USA.
[g]Department of Periodontics and Oral Medicine, School of Dentistry, University of Michigan, Ann Arbor, MI, USA.

Received for publication Jul 7, 2015; returned for revision Oct 6, 2015; accepted for publication Oct 12, 2015.

2212-4403/$ - see front matter
http://dx.doi.org/10.1016/j.oooo.2015.10.015

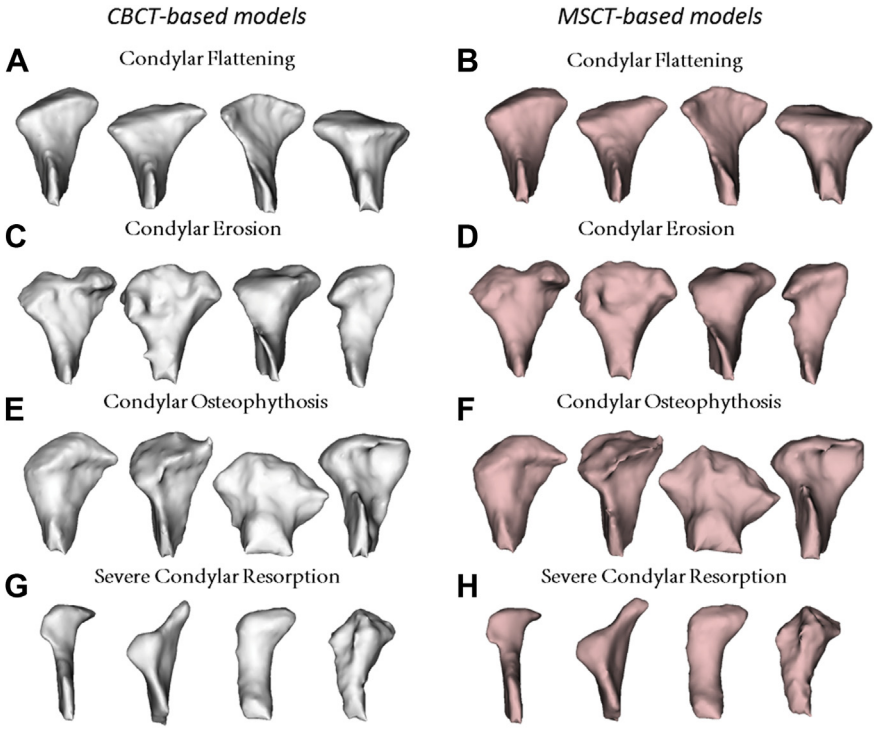

Fig. 1. CBCT- and MSCT-based models of condyles diagnosed with chronic TMJ osteoarthritis. Osteoarthritic surface changes in the study included condylar flattening (**A**, **B**), erosion (**C**, **D**), osteophythosis (**E**, **F**), and severe condylar resorption (**G**, **H**).

used.[9,13] Although some authors have stated that high-resolution images (voxel size smaller than .2 mm) provide significantly more accurate diagnoses,[14-20] others did not find differences among voxel sizes ranging from .125 to .4 mm for most clinical purposes.[21-28] It has been shown that a .3-mm voxel size associates good diagnostic performance with lower X-ray exposure.[29-31] However, further clinical studies are needed to better understand specific protocols for different diagnostic tasks.[32,33]

New technologies, such as the use of CBCT-based surface models, allow for comprehensive qualitative and quantitative evaluations of the overall TMJ morphologic alterations.[2] Three-dimensional shape-correspondence analysis (SPHARM-PDM) has been described as a method to precisely locate and quantify morphologic changes between healthy and pathologic structures.[34,35] This innovative method for diagnosing TMJ osteoarthritis potentially minimizes the importance of the examiner's experience, reducing intra- and interrater related errors, standardizes findings, and contributes to the development of new imaging markers for risk factors.[5]

While CBCT has been shown to provide novel 3-D research data and clinically relevant diagnostic and treatment-planning information,[2,5] its validity as a reliable tool compared with MSCT data is still questionable. Surgeons have often preferred MSCT data to produce anatomically accurate stereolithographic models of the jaws and joints through rapid prototyping technology systems.[36-41] This study tested the diagnostic hypothesis that CBCT-based 3-D condylar surface models are reliably comparable to MSCT. Therefore, we quantitatively compared assessments of mandibular condyle morphology using CBCT and MSCT virtual 3-D surface models.

MATERIALS AND METHODS

This study is a secondary data analysis of available CBCT and MSCT scans obtained for clinical purposes from 74 patients (146 mandibular condyles) diagnosed with chronic TMJ OA (Figure 1). Two condyles were excluded from the study due to the presence of unilateral TMJ prostheses. CBCT scans were taken as a diagnostic clinical record for detecting TMJ morphologic changes in patients with clinical symptoms of TMJ OA using diagnostic criteria for temporomandibular disorders.[42] A 17 × 23 cm extended field of view image-acquisition protocol was used during an 8.9-second scan, with an isotropic .3 mm voxel size (i-Cat® CBCT, 120 kV, 5 mA, Imaging Sciences, Hatfield, PA). The treatment plan for the patients included in this study involved condylar resection and prosthetic joint replacement of at least one of the TMJs. The precise custom-fitted fabrication of a total TMJ joint prosthesis required a MSCT scan (LightSpeed16® MultiSlice CT Scanner, 120 kV, 180 mA, 1.0 pitch, 512.512 matrix size, .625-mm slice

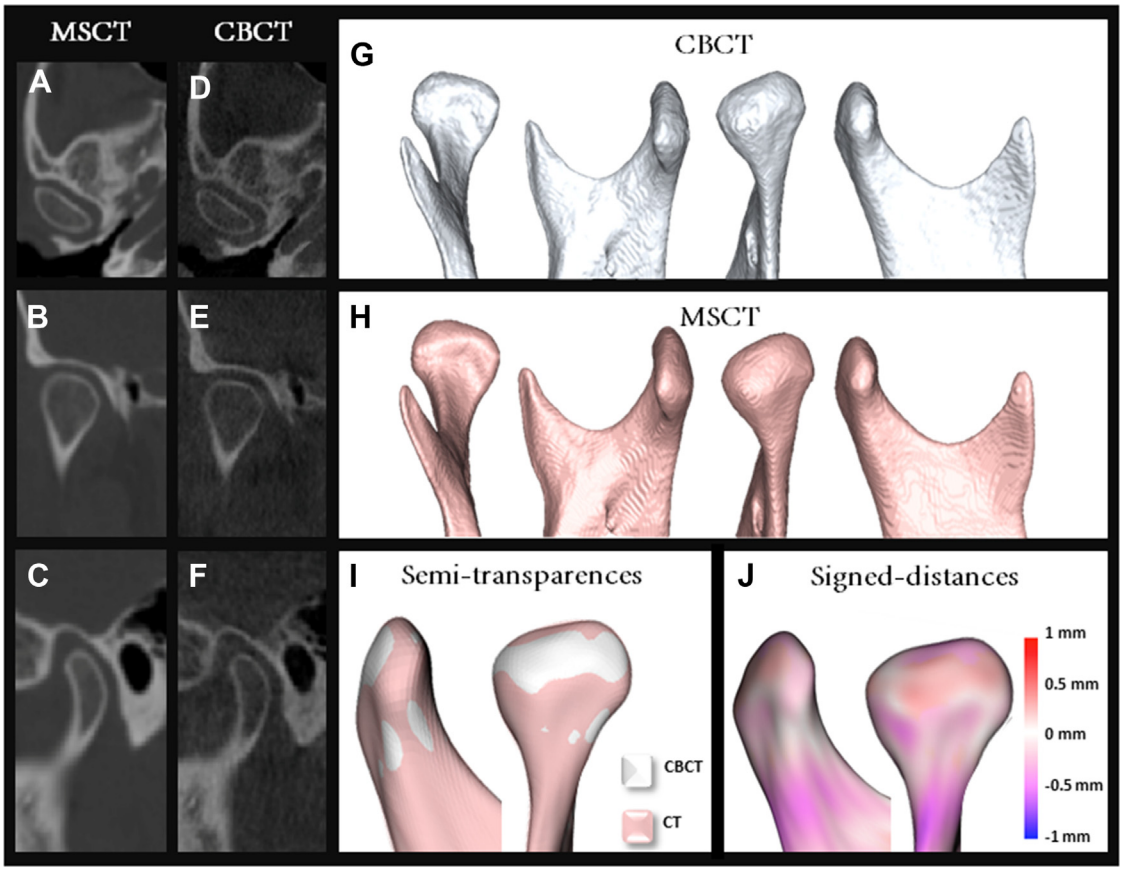

Fig. 2. Construction of 3-D surface models of the right condyle from cone beam computed tomography (CBCT) and multislice spiral computed tomography (MSCT) greyscale images of a patient. **A**, **B**, and **C** show MSCT multiplanar images: axial (**A**), coronal (**B**) and sagittal (**C**) views; **D**, **E**, and **F** show CBCT multiplanar images: axial (**D**), coronal (**E**), and sagittal (**F**) views; **G** and **H** show frontal, medial, posterior, and lateral views of the right condyles rendered respectively from the CBCT and MSCT greyscale images. **I**, Semitransparent overlays of the registered surface models. **J**, Color-coded maps displaying the computed differences between 4002 corresponding points in the condylar surface constructed from MSCT and CBCT models. For this condyle, the maximum difference observed was .48 mm and the 50th, 75th, and 95th percentiles were, respectively, .21 mm, .29 mm, and .29 mm.

thickness, pixel size of .390, resolution of 2.564 pixels per mm, GE Medical Systems, Milwaukee, WI). Each device was made using computer-aided design/computer-aided manufacturing (CAD/CAM) technology to construct a 3-D stereolithographic model of the TMJ and associated bony structures. The secondary data analysis of de-identified CBCT and MSCT scans in this study was approved by the university institutional review board and is in compliance with the Helsinki Declaration.

A total of 292 3-D surface models of the condyles were constructed from each CBCT (146 condyles) and MSCT scans (146 condyles). The cortical boundaries of the condylar region visible in the cross sections of volumetric data sets were outlined using a semi-automatic segmentation procedure. Thus, after selecting the region of interest, the program automatically segmented the mandibular condyle and part of the ramus region. The operator was then able to check out slice-by-slice the effectiveness of the automatic segmentation and perform manual editing in the three planes of space. Such an approach combined the efficiency and repeatability of automatic segmentation with the sound judgment of human expertise (ITK-SNAP software v.2.4, www.itksnap.org) (Figure 2A-H).[43,44]

After generation of the 3-D surface models, left condyles were mirrored in the sagittal plane to form right condyles to facilitate comparisons (Figure 3A). All CBCT-based models were consistently approximated to a chosen reference condyle to establish a common co-ordinate system within the 3-D space (Figure 3B) and make it possible to create average CBCT and MSCT-based condylar models. For a paired comparison, the homologous CBCT and MSCT images were also registered relative to each other using regional voxel-based registration, and the anisotropic

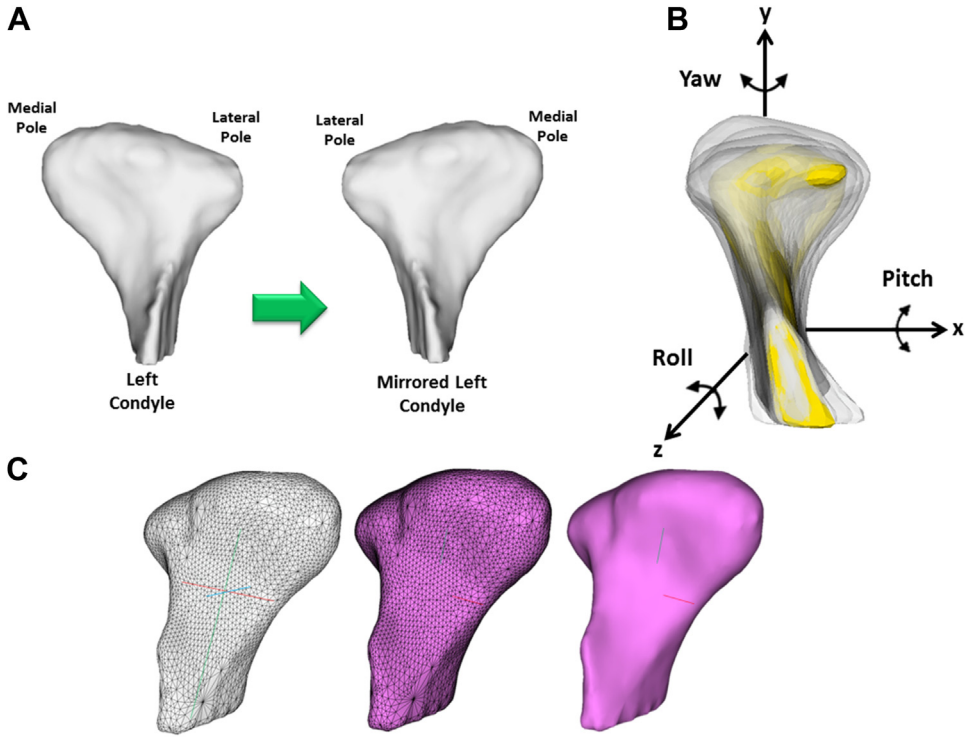

Fig. 3. **A**, All left condyles were mirrored as right condyles, making possible the superimposition and construction of the average condylar morphology for both CBCT- and MSCT-based models. **B**, Reference condylar model (yellow) with the overlay of multiple condyles approximated in the same coordinate system. **C**, Parameterization of 4002 corresponding surface mesh points for statistical comparisons and detailed morphologic characterization.

voxels of the MSCT scans were automatically reformatted to .3-mm isotropic voxels. Thus, the greyscale intensity of each voxel in the MSCT was registered to the CBCT images.

After registration, all models were simultaneously cropped to obtain the condylar region of interest. Shape-correspondence analysis (SPHARM-PDM software, http://www.nitrc.org/projects/spharm-pdm) was used to generate a mesh approximation from the volumes, establishing correspondence between each of the 4002 points in the condylar surface models across all patients from both image modalities (Figure 3C). An average 3-D condylar shape was then generated for the CBCT and the MSCT groups (Linux MeshMath script).

The Linux MeshMath script was then used to calculate 3-D pointwise subtractions between each homologous CBCT and MSCT corresponding condylar surface models, and also between the group average condylar surface models. Semitransparent overlays between the average models were used to visually compare the two groups in the 3-D slicer software (www.slicer.org). The computed 4002 vector differences were displayed as corresponding signed surface distances on each comparable condylar surface (Figures 2I and 2J).

Intra- and interobserver errors in segmentation of the mandibular condyles were tested by two calibrated observers, using a randomly selected sample of 10 CBCT and 10 MSCT volumetric data sets. Systematic differences between the observers were assessed using a Hotelling T^2 test in a multivariate analysis of covariance software (ShapeAnalysisMANCOVA).[45]

The statistical framework for testing pairwise and group differences between CBCT- and MSCT-based condylar models also included ShapeAnalysisMANCOVA. Results were analyzed by using corresponding absolute distances, *i.e.*, the magnitude of the differences between the models in each surface point. Statistical significance is graphically displayed in the average surface model using color-coded maps: highly significant differences ($P < .01$) would be color coded in red, intermediately significant differences would vary from yellow to green ($.01 > P > .05$), and nonsignificant differences would be color coded in blue ($P > .05$). Descriptive statistics of mean, standard deviation, median, 75th and 95th percentiles, and maximum and minimum differences were also calculated for each pairwise comparison. A one-sample t test was conducted to evaluate whether the absolute mean differences between each CBCT- and MSCT-based model were statistically significantly different than .5 mm.

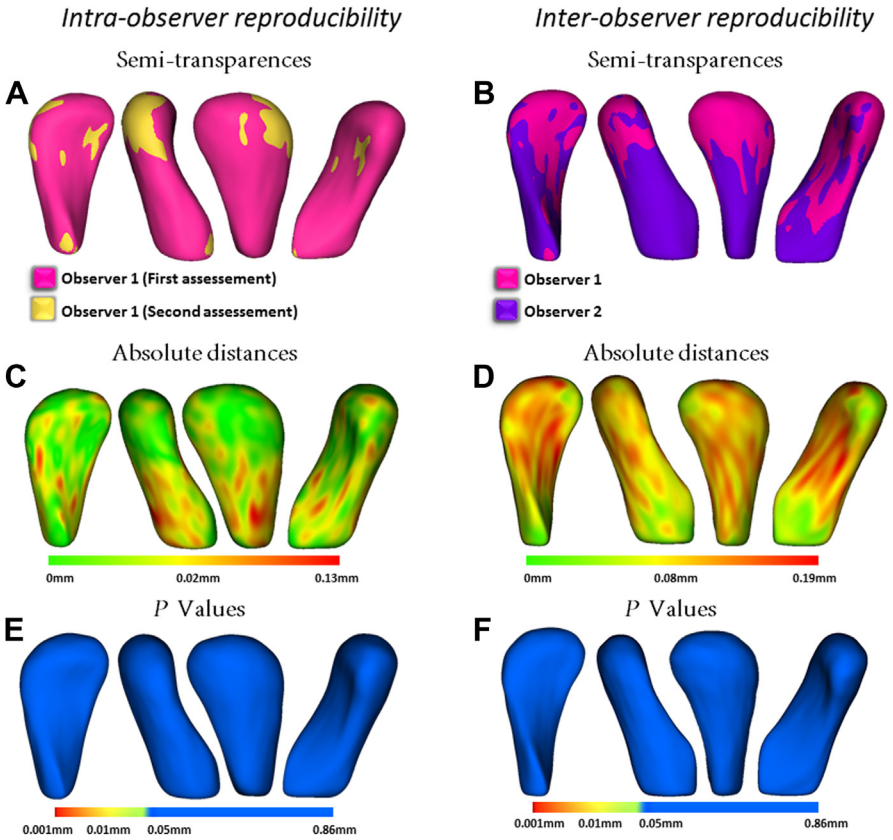

Fig. 4. Intra- and interobserver reproducibility results. **A** and **B**, Overlay of the average models constructed by the observers for 10 cone beam computed tomography and 10 multislice spiral computed tomography images randomly selected. **C** and **D**, Absolute-distances map obtained after subtracting the average models constructed from the segmentations of two independent observers. **E** and **F**, Significance map shows $P > .05$ for the whole condylar surface considering both intra- and interobserver reproducibility.

To exclude possible outliers, this test considered the 95th percentile data. All the tests were conducted with 5% significance levels.

RESULTS

The largest intra- and interobserver differences were .15 mm (mean .07 mm; SD .02) and .19 mm (mean .10 mm; SD .03) respectively. These differences were found between the average models derived from each observer's condyle segmentations of both CBCT and MSCT scans. The significance maps showed no statistically significant differences for any of the 4002 points in study during both intra- ($P > .88$) and interobserver reproducibility ($P > .73$) (Figure 4).

Descriptive statistics of the absolute differences observed between paired CBCT- and MSCT-based models are summarized in Table I and Figure 5. For each one of the 146 pairs of condyles in this study, the mean differences observed between the 4002 corresponding points on the surface of CBCT- and MSCT-based models ranged from .15 mm to 1.12 mm (mean .41 mm; SD .17; 95% confidence interval [CI] .38 to .44). Considering all the differences between each corresponding 4002 points in 146 condylar surface models, a total of 584,292 comparisons, the largest difference observed was 2.55 mm. The 95th percentile showed that at 95% of the condylar surface the differences observed were below .52 mm (SD .25; 95% CI .48 to .56).

Figures 6A and B show, respectively, the semitransparencies and the absolute-distances color-coded map obtained from the comparison between the average CBCT- and MSCT-based models. The distances observed in the color-coded map were determined by subtracting each one of the 4002 corresponding surface points on average CBCT from the average MSCT condyle. ShapeAnalysisMANCOVA showed no statistically significant difference between the groups ($P > .68$). A 3-D visualization of the absence of statistically significant differences is presented in Figure 6C, where nonsignificant differences are color coded in blue ($P > .05$).

The one-sample t test showed that the 95% CIs of the absolute mean differences between each paired CBCT- and MSCT-based model were not statistically significantly greater than .5 mm ($P = .411$; mean difference of .02 mm; 95% CI −.02 to .06; as shown in Table II).

Table I. Descriptive statistics of the differences between cone beam computed tomography (CBCT)- and multislice spiral computed tomography (MSCT)-based models

					Percentile*			
N	*Mean**	*SD**	*Minimum**	*Maximum**	*50th (Median)*	*75th*	*95th*	*Significance†*
146	.41 (.15-1.12)	.17 (.07-.48)	.03 (0‡-.19)	1.01 (.39-2.55‡)	.39 (.14-1.13)	.52 (.19-1.43)	.52 (.19-1.43)	$P > .68$

*Values obtained from the mean differences observed for each of the 146 condyles (4,002 points) (range in parentheses).
†Value obtained from the comparison between the average CBCT- and MSCT-based models.
‡Values refer to the minimum and maximum differences observed considering each one of the points in the surface models for all patients in this study (584.292 corresponding points).

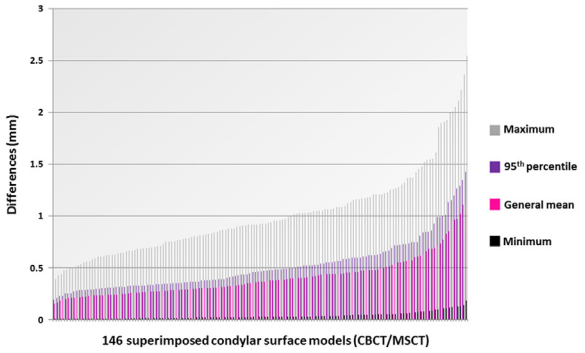

Fig. 5. Differences observed between CBCT- and MSCT-based models.

DISCUSSION

This study compared quantitative assessments of 3-D mandibular condyle morphology using CBCT and MSCT scans taken for clinical purposes. CBCT has revolutionized diagnosis and treatment planning in the field of craniofacial disorders, particularly in the assessment of TMJ bony alterations. The lower radiation dose and cost compared with MSCT provide clinicians and researchers with a valuable diagnostic tool for identifying specific changes in the morphology of the mandibular condyles with osteoarthritis.[1,4,6-8] However, for planning surgical interventions with stereolithographic technology, a MSCT is still often acquired.[36-41,46]

Previous studies have compared CBCT and MSCT images for different medical and dental applications. Those studies utilized linear measurements obtained from axial, coronal, and sagittal slices, 2-D measurements based on 3-D rendering, or volume differences.[47-52] Other investigations specifically comparing CBCT and MSCT images of the TMJ condyles were also limited to assessment of the 2-D multiplanar cross sections or to subjective evaluations.[19,33,53-56] The current paper is the first clinical study to quantitatively compare whole 3-D mandibular condyle surfaces constructed from CBCT and MSCT scans. The 3-D surface models provide additional diagnostic information on size, shape, and exact location of the bone abnormality on the affected joint.[2,5,6,34,57]

This study did not utilize an absolute geometric ground truth to evaluate the quality of CBCT imaging, and instead used the MSCT scans as a clinically established method of reference.[53,58-62] Therefore, the mandibular condyle models generated from CBCT scans were compared with MSCT-based models of the same structures, which were considered as the gold standard. In the present study, the models were constructed through a semiautomatic discrimination procedure, by examiners previously calibrated with other scans not included in this study. Our results showed excellent intra- and interobserver reliability of the segmentation procedures, which corroborates other authors' findings.[5,63-65] These images were analyzed at a .3-mm isotropic voxel size, which has been considered as an appropriate resolution for most clinical purposes.[29] Moreover, the anatomic correspondence between 4002 points in each set of homologous CBCT and MSCT models was automatically established by voxel-based registration and quantified by SPHARM-PDM, which are observer-independent tools. Thus, our results were not confounded by examiner subjectivity.

The image-analysis procedures in this study utilized voxelwise rigid registration and shape correspondence to quantify the differences between 3-D surface models constructed from CBCT and MSCT. The fully automated superimposition using voxelwise rigid registration between CBCT and MSCT scans in this study does not depend on landmarks or planes and, rather, compared the selected reference structures voxel by voxel, achieving the least grayscale density difference between the two images. Previous studies have shown that this method provides high accuracy in 3-D registration.[57,66,67] Likewise, the surface parametrization method employed in this study, the SPHARM-PDM shape analysis toolbox,[68] has been shown to provide a unique and symmetric point-to-point correspondence across all measured surfaces. In the present study, shape differences were calculated between each corresponding point on CBCT- and MSCT-based models, and statistical shape analysis allowed for a localized analysis of shape *via* multivariate analysis of covariance (MANCOVA). After correspondence establishment

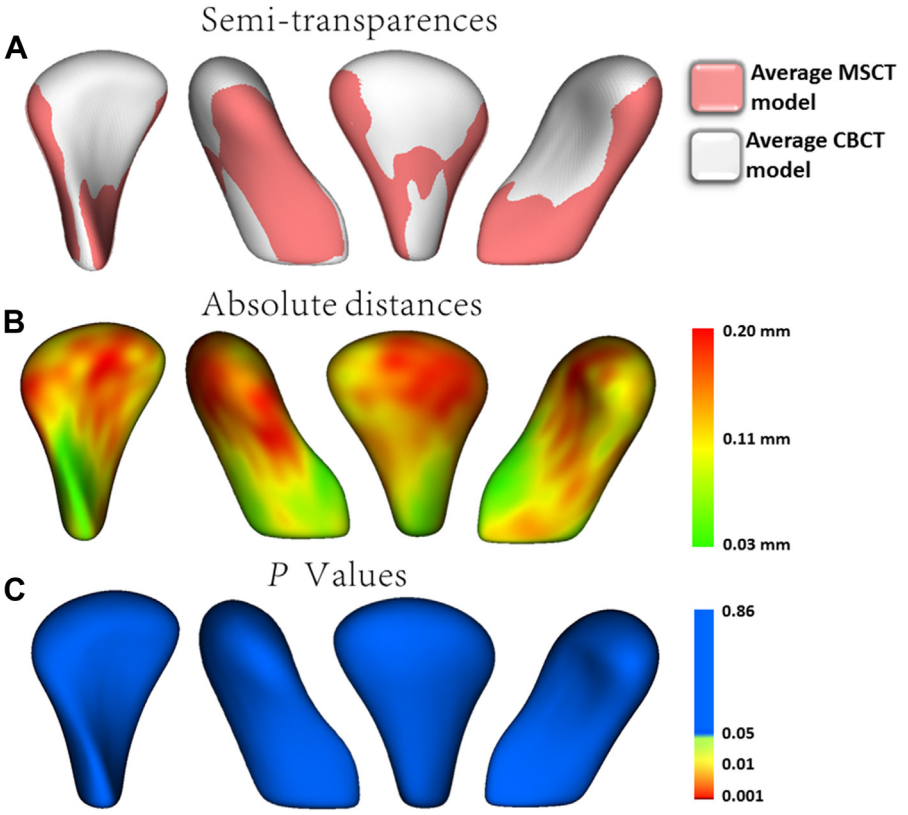

Fig. 6. **A**, Semitransparencies showing the superimposition of the average CBCT- and MSCT-based models. **B**, Absolute distances obtained after subtracting the average models. **C**, Significance map shows $P > .05$ for the whole condylar surface.

Table II. One-sample t test for the null hypothesis that the differences observed between CBCT- and MSCT-based models were .5 mm

			Test value = .5					
							95% CI of the difference	
N	Mean	SD	t	Difference	Significance	Mean difference	Lower	Upper
146	.52	.24	.82	145	.41	.02	−.02	.06

CI, condifence interval.

using SPHARM-PDM,[68,69] alignment, and scaling normalization in a shape population, the traditional statistical analysis approach consisted of testing for differences between groups at every surface location.[70] This method has been validated as an accurate tool for localizing and quantifying the degree of morphologic mandibular condylar changes.[34]

This study results showed that the mean differences between paired comparisons of CBCT- and MSCT-based models were at a sub-mm level, except for three condyles that showed mean differences greater than 1 mm and smaller than 1.12 mm. Taking into account all the 584,292 differences between corresponding points in this study, only one condyle presented with maximum point difference of 2.55 mm (Figure 5). While the overall mean difference for all condyles was .41 mm, the 95th percentile was only slightly larger, .52 mm (Table I, Figure 5). Nine condyles that presented with severe condylar changes showed 95th percentile differences ranging from 1 mm to 1.43 mm. These morphologic abnormalities possibly made the segmentation procedure more challenging and prone to larger errors.

The use of .3-mm isotropic voxel size CBCT scans in this study has been previously justified in the literature, even though not specifically for assessments of 3-D condylar dysmorphology. Patel et al. observed that the agreement between CBCT and physical truth measurements are not significantly different with the use of .2 mm or .4 mm voxel size,[31] and Primo et al. reported no significant differences between maxillofacial prototypes produced from CBCT data with .25 mm and .4 mm voxel sizes on one hand and MSCT data with .3 mm pixel size on the other.[28] Other specific assessments of erosive condylar changes[19] have reported only findings at the 2-D multiplanar views, where cross-sectional slices of CBCT images acquired using a 6-inch field of view at a voxel size of .2 mm presented significantly better image quality than CBCT

scans acquired using a 12-inch field of view with a voxel size of .4 mm. However, those findings referred to the quality of the greyscale images and not the 3-D condylar surface models constructed from the scans and assessed in this study.

The accuracy of CBCT scans in detecting TMJ osteoarthritic changes has been previously tested using dry skulls with simulated bone defects or phantoms, which do not fully reproduce clinical conditions.[19,33,53-55] The present study revealed that the mean differences between CBCT- and MSCT-based models were found to be around 0.5 mm, which has been considered adequate precision for most clinical applications.[31,34,66,71,72] This study assessed 3-D morphologic changes that occur in the mandibular condyle surface, such as erosion, flattening, and osteophytosis; however, it did not evaluate internal bony alterations of degenerative arthritis, such as increased sclerosis or the presence of subchondral cysts. Further studies are required to investigate the detection of clinically relevant subchondral changes in CBCT and MSCT.

CONCLUSION

The present findings indicate that CBCT-based models are comparable to those derived from MSCT scans in identifying some of the changes associated with OA in the mandibular condyle. 3-D virtual surface models constructed from CBCT scans may be considered as reliable tools for the assessment of condylar morphology.

REFERENCES

1. Mozzo P, Procacci C, Tacconi A, Martini PT, Andreis IA. A new volumetric CT machine for dental imaging based on the cone-beam technique: Preliminary results. *Eur Radiol*. 1998;8:1558-1564.
2. Kapila SD, Nervina JM. CBCT in orthodontics: Assessment of treatment outcomes and indications for its use. *Dentomaxillofac Radiol*. 2015;44:20140282.
3. Ahmad M, Hollender L, Anderson Q, et al. Research diagnostic criteria for temporomandibular disorders (RDC/TMD): Development of image analysis criteria and examiner reliability for image analysis. *Oral Surg Oral Med Oral Pathol Oral Radiol Endod*. 2009;107:844-860.
4. Alexiou K, Stamatakis H, Tsiklakis K. Evaluation of the severity of temporomandibular joint osteoarthritic changes related to age using cone beam computed tomography. *Dentomaxillofac Radiol*. 2009;38:141-147.
5. Cevidanes LH, Hajati AK, Paniagua B, et al. Quantification of condylar resorption in temporomandibular joint osteoarthritis. *Oral Surg Oral Med Oral Pathol Oral Radiol Endod*. 2010;110:110-117.
6. Cevidanes LH, Bailey LJ, Tucker GR Jr, et al. Superimposition of 3 D cone-beam CT models of orthognathic surgery patients. *Dentomaxillofac Radiol*. 2005;34:369-375.
7. Ludlow JB, Davies-Ludlow LE, Brooks SL. Dosimetry of two extraoral direct digital imaging devices: NewTom cone beam CT and Orthophos Plus DS panoramic unit. *Dentomaxillofac Radiol*. 2003;32:229-234.
8. Mah J, Hatcher D. Three-dimensional craniofacial imaging. *Am J Orthod Dentofacial Orthop*. 2004;126:308-309.
9. Lukat TD, Perschbacher SE, Pharoah MJ, Lam EW. The effects of voxel size on cone beam computed tomography images of the temporomandibular joints. *Oral Surg Oral Med Oral Pathol Oral Radiol*. 2015;119:229-237.
10. Thonissen P, Ermer MA, Schmelzeisen R, et al. Sensitivity and specificity of cone beam computed tomography in thin bony structures in maxillofacial surgery—A clinical trial. *J Craniomaxillofac Surg*. 2015;43:1284-1288.
11. Scarfe WC, Li Z, Aboelmaaty W, Scott SA, Farman AG. Maxillofacial cone beam computed tomography: Essence, elements and steps to interpretation. *Aust Dent J*. 2012;57(suppl 1):46-60.
12. Scarfe WC, Farman AG. What is cone-beam CT and how does it work? *Dent Clin N Am*. 2008;52:707-730.
13. Kamburoğlu K, Ereş G, Akgün C, Yeta EN, Gülen O, Karacaoğlu F. Effect of voxel size on accuracy of cone beam computed tomography-aided assessment of periodontal furcation involvement. *Oral Surg Oral Med Oral Pathol Oral Radiol*. 2015;120:644-650.
14. Sun Z, Smith T, Kortam S, et al. Effect of bone thickness on alveolar bone-height measurements from cone-beam computed tomography images. *Am J Orthod Dentofacial Orthop*. 2011;139:e117-e127.
15. Wenzel A, Haiter-Neto F, Frydenberg M, Kirkevang LL. Variable-resolution cone-beam computerized tomography with enhancement filtration compared with intraoral photostimulable phosphor radiography in detection of transverse root fractures in an in vitro model. *Oral Surg Oral Med Oral Pathol Oral Radiol Endod*. 2009;108:939-945.
16. Melo SL, Bortoluzzi EA, Abreu M Jr, Correa LR, Correa M. Diagnostic ability of a cone-beam computed tomography scan to assess longitudinal root fractures in prosthetically treated teeth. *J Endod*. 2010;36:1879-1882.
17. Dalili Z, Taramsari M, Mousavi Mehr SZ, Salamat F. Diagnostic value of two modes of cone-beam computed tomography in evaluation of simulated external root resorption: An in vitro study. *Imaging Sci Dent*. 2012;42:19-24.
18. Kamburoglu K, Kursun S. A comparison of the diagnostic accuracy of CBCT images of different voxel resolutions used to detect simulated small internal resorption cavities. *Int Endod J*. 2010;43:798-807.
19. Librizzi ZT, Tadinada AS, Valiyaparambil JV, Lurie AG, Mallya SM. Cone-beam computed tomography to detect erosions of the temporomandibular joint: Effect of field of view and voxel size on diagnostic efficacy and effective dose. *Am J Orthod Dentofacial Orthop*. 2011;140:e25-e30.
20. Haiter-Neto F, Wenzel A, Gotfredsen E. Diagnostic accuracy of cone beam computed tomography scans compared with intraoral image modalities for detection of caries lesions. *Dentomaxillofac Radiol*. 2008;37:18-22.
21. Ozer SY. Detection of vertical root fractures by using cone beam computed tomography with variable voxel sizes in an in vitro model. *J Endod*. 2011;37:75-79.
22. da Silveira PF, Vizzotto MB, Liedke GS, et al. Detection of vertical root fractures by conventional radiographic examination and cone beam computed tomography—An in vitro analysis. *Dent Traumatol*. 2013;29:41-46.
23. Liedke GS, da Silveira HE, da Silveira HL, Dutra V, de Figueiredo JA. Influence of voxel size in the diagnostic ability of cone beam tomography to evaluate simulated external root resorption. *J Endod*. 2009;35:233-235.
24. Kamburoglu K, Murat S, Yuksel SP, Cebeci AR, Paksoy CS. Occlusal caries detection by using a cone-beam CT with different

voxel resolutions and a digital intraoral sensor. *Oral Surg Oral Med Oral Pathol Oral Radiol Endod*. 2010;109:e63-e69.
25. Patcas R, Muller L, Ullrich O, Peltomaki T. Accuracy of cone-beam computed tomography at different resolutions assessed on the bony covering of the mandibular anterior teeth. *Am J Orthod Dentofacial Orthop*. 2012;141:41-50.
26. Torres MG, Campos PS, Segundo NP, Navarro M, Crusoe-Rebello I. Accuracy of linear measurements in cone beam computed tomography with different voxel sizes. *Implant Dent*. 2012;21:150-155.
27. Sherrard JF, Rossouw PE, Benson BW, Carrillo R, Buschang PH. Accuracy and reliability of tooth and root lengths measured on cone-beam computed tomographs. *Am J Orthod Dentofacial Orthop*. 2010;137(suppl 4):S100-S108.
28. Primo BT, Presotto AC, de Oliveira HW, et al. Accuracy assessment of prototypes produced using multi-slice and cone-beam computed tomography. *Int J Oral Maxillofac Surg*. 2012;41:1291-1295.
29. Waltrick KB, Nunes de Abreu MJ Junior, Correa M, Zastrow MD, Dutra VD. Accuracy of linear measurements and visibility of the mandibular canal of cone-beam computed tomography images with different voxel sizes: An in vitro study. *J Periodontol*. 2013;84:68-77.
30. Hekmatian E, Jafari-Pozve N, Khorrami L. The effect of voxel size on the measurement of mandibular thickness in cone-beam computed tomography. *Dent Res J (Isfahan)*. 2014;11:544-548.
31. Patel A, Tee BC, Fields H, et al. Evaluation of cone-beam computed tomography in the diagnosis of simulated small osseous defects in the mandibular condyle. *Am J Orthod Dentofacial Orthop*. 2014;145:143-156.
32. Spin-Neto R, Gotfredsen E, Wenzel A. Impact of voxel size variation on CBCT-based diagnostic outcome in dentistry: A systematic review. *J Digit Imaging*. 2013;26:813-820.
33. Bastos LC, Campos PS, Ramos-Perez FM, Pontual Ados A, Almeida SM. Evaluation of condyle defects using different reconstruction protocols of cone-beam computed tomography. *Braz Oral Res*. 2013;27:503-509.
34. Paniagua B, Cevidanes L, Walker D, et al. Clinical application of SPHARM-PDM to quantify temporomandibular joint osteoarthritis. *Comput Med Imaging Graph*. 2011;35:345-352.
35. Neuroimaging Informatics Tools and Resources Clearinghouse. Projects Spharm-PDM. Available at: http://www.nitrc.org/projects/spharm-pdm. Accessed October 27, 2015.
36. Dolwick MF. Temporomandibular joint surgery for internal derangement. *Dent Clin North Am*. 2007;51:195-208.
37. Guarda-Nardini L, Manfredini D, Ferronato G. Temporomandibular joint total replacement prosthesis: Current knowledge and considerations for the future. *Int J Oral Maxillofac Surg*. 2008;37:103-110.
38. Mercuri LG, Wolford LM, Sanders B, et al. Custom CAD/CAM total temporomandibular joint reconstruction system: Preliminary multicenter report. *J Oral Maxillofac Surg*. 1995;53:106-115.
39. Wolford LM. Temporomandibular joint devices: Treatment factors and outcomes. *Oral Surg Oral Med Oral Pathol Oral Radiol Endod*. 1997;83:143-149.
40. Wolford LM, Pitta MC, Reiche-Fischel O, Franco PF. TMJ Concepts/Techmedica custom-made TMJ total joint prosthesis: 5-year follow-up study. *Int J Oral Maxillofac Surg*. 2003;32:268-274.
41. Wolford LM, Dingwerth DJ, Talwar RM, Pitta MC. Comparison of 2 temporomandibular joint total joint prosthesis systems. *J Oral Maxillofac Surg*. 2003;61:685-690.
42. Schiffman E, Ohrbach R, Truelove E, et al. Diagnostic criteria for temporomandibular disorders (DC/TMD) for clinical and research applications: Recommendations of the International RDC/TMD Consortium Network* and Orofacial Pain Special Interest Group. *J Oral Facial Pain Headache*. 2014;28:6-27.
43. Itk-SNAP. Penn Image Computing and Science Laboratory. Available at: http://www.itksnap.org. Accessed April 17, 2014.
44. Yushkevich PA, Piven J, Hazlett HC, et al. User-guided 3 D active contour segmentation of anatomical structures: Significantly improved efficiency and reliability. *Neuroimage*. 2006;31:1116-1128.
45. Neuroimaging Informatics Tools and Resources Clearinghouse. shapeAnalysisMANCOVA - SPHARM tools. Available at: http://www.nitrc.org/projects/shape_mancova. Accessed October 27, 2015.
46. Ingawale S, Goswami T. Temporomandibular joint: Disorders, treatments, and biomechanics. *Ann Biomed Eng*. 2009;37:976-996.
47. Dahmani-Causse M, Marx M, Deguine O, et al. Morphologic examination of the temporal bone by cone beam computed tomography: Comparison with multislice helical computed tomography. *Eur Ann Otorhinolaryngol Head Neck Dis*. 2011;128:230-235.
48. Loubele M, Van Assche N, Carpentier K, et al. Comparative localized linear accuracy of small-field cone-beam CT and multislice CT for alveolar bone measurements. *Oral Surg Oral Med Oral Pathol Oral Radiol Endod*. 2008;105:512-518.
49. Medelnik J, Hertrich K, Steinhauser-Andresen S, Hirschfelder U, Hofmann E. Accuracy of anatomical landmark identification using different CBCT- and MSCT-based 3 D images: An in vitro study. *J Orofac Orthop*. 2011;72:261-278.
50. Patcas R, Markic G, Muller L, et al. Accuracy of linear intraoral measurements using cone beam CT and multidetector CT: A tale of two CTs. *Dentomaxillofac Radiol*. 2012;41:637-644.
51. Pellerin O, Lin M, Bhagat N, et al. Comparison of semi-automatic volumetric VX2 hepatic tumor segmentation from cone beam CT and multi-detector CT with histology in rabbit models. *Acad Radiol*. 2013;20:115-121.
52. Poeschl PW, Schmidt N, Guevara-Rojas G, et al. Comparison of cone-beam and conventional multislice computed tomography for image-guided dental implant planning. *Clin Oral Investig*. 2013;17:317-324.
53. Hintze H, Wiese M, Wenzel A. Cone beam CT and conventional tomography for the detection of morphological temporomandibular joint changes. *Dentomaxillofac Radiol*. 2007;36:192-197.
54. Honda K, Larheim TA, Maruhashi K, Matsumoto K, Iwai K. Osseous abnormalities of the mandibular condyle: Diagnostic reliability of cone beam computed tomography compared with helical computed tomography based on an autopsy material. *Dentomaxillofac Radiol*. 2006;35:152-157.
55. Katakami K, Shimoda S, Kobayashi K, Kawasaki K. Histological investigation of osseous changes of mandibular condyles with backscattered electron images. *Dentomaxillofac Radiol*. 2008;37:330-339.
56. Zain-Alabdeen EH, Alsadhan RI. A comparative study of accuracy of detection of surface osseous changes in the temporomandibular joint using multidetector CT and cone beam CT. *Dentomaxillofac Radiol*. 2012;41:185-191.
57. Cevidanes LH, Styner MA, Proffit WR. Image analysis and superimposition of 3-dimensional cone-beam computed tomography models. *Am J Orthod Dentofacial Orthop*. 2006;129:611-618.
58. Cara AC, Gaia BF, Perrella A, et al. Validity of single- and multislice CT for assessment of mandibular condyle lesions. *Dentomaxillofac Radiol*. 2007;36:24-27.
59. Marques AP, Perrella A, Arita ES, Pereira MF, de Gusmão Paraíso Cavalcanti M. Assessment of simulated mandibular condyle bone lesions by cone beam computed tomography. *Braz Oral Res*. 2010;24:467-474.

60. Perrella A, Borsatti MA, Tortamano IP, Rocha RG, Cavalcanti MG. Validation of computed tomography protocols for simulated mandibular lesions: A comparison study. *Braz Oral Res*. 2007;21:165-169.
61. Tsuruta A, Yamada K, Hanada K, et al. Thickness of the roof of the glenoid fossa and condylar bone change: A CT study. *Dentomaxillofac Radiol*. 2003;32:217-221.
62. Yamada K, Tsuruta A, Hanada K, Hayashi T. Morphology of the articular eminence in temporomandibular joints and condylar bone change. *J Oral Rehabil*. 2004;31:438-444.
63. Fourie Z, Damstra J, Schepers RH, Gerrits PO, Ren Y. Segmentation process significantly influences the accuracy of 3 D surface models derived from cone beam computed tomography. *Eur J Radiol*. 2012;81:e524-e530.
64. Luu NS, Mandich MA, Flores-Mir C, et al. The validity, reliability, and time requirement of study model analysis using cone-beam computed tomography-generated virtual study models. *Orthod Craniofac Res*. 2014;17:14-26.
65. Xi T, van Loon B, Fudalej P, et al. Validation of a novel semi-automated method for three-dimensional surface rendering of condyles using cone beam computed tomography data. *Int J Oral Maxillofac Surg*. 2013;42:1023-1029.
66. Almukhtar A, Ju X, Khambay B, McDonald J, Ayoub A. Comparison of the accuracy of voxel based registration and surface based registration for 3 D assessment of surgical change following orthognathic surgery. *PLoS One*. 2014;9:e93402.
67. Nada RM, Maal TJ, Breuning KH, et al. Accuracy and reproducibility of voxel based superimposition of cone beam computed tomography models on the anterior cranial base and the zygomatic arches. *PLoS One*. 2011;6:e16520.
68. Styner M, Oguz I, Xu S, et al. Framework for the Statistical Shape Analysis of Brain Structures using SPHARM-PDM. *Insight J*. 2006:242-250.
69. Brechbuhler C, Gerig G, Kubler O. Parameterization of closed surfaces for 3 d shape description. *Comp Vision Image Under*. 1995;61:154-170.
70. Paniagua B, Styner M, Macenko M, Pantazis D, Niethammer M. Local shape analysis using MANCOVA. *Insight J*. 2009:21.
71. Bell A, Ayoub AF, Siebert P. Assessment of the accuracy of a three-dimensional imaging system for archiving dental study models. *J Orthod*. 2003;30:219-223.
72. Bettega G, Cinquin P, Lebeau J, Raphael B. Computer-assisted orthognathic surgery: Clinical evaluation of a mandibular condyle repositioning system. *J Oral Maxillofac Surg*. 2002;60:27-34.

Reprint requests:

Liliane Rosas Gomes, DDS, MS, PhD student
Faculdade de Odontologia de Araraquara
UNESP Universidade Estadual Paulista
Rua Humaitá
1680, CEP: 14801-903
Araraquara
São Paulo
Brasil
lilianerosas@hotmail.com